Theoretical study of the synthesis of superheavy nuclei with $Z = 119$ and 120 in heavy-ion reactions with trans-uranium targets

Nan Wang,[1] En-Guang Zhao,[2,3,4] Werner Scheid,[5] and Shan-Gui Zhou[2,3,*]

[1] *College of Physics, Shenzhen University, Shenzhen 518060, China*
[2] *State Key Laboratory of Theoretical Physics, Institute of Theoretical Physics, Chinese Academy of Sciences, Beijing 100190, China*
[3] *Center of Theoretical Nuclear Physics, National Laboratory of Heavy Ion Accelerator, Lanzhou 730000, China*
[4] *School of Physics, Peking University, Beijing 100871, China*
[5] *Institut für Theoretische Physik der Justus-Liebig-Universität, D-35392 Giessen, Germany*

(Dated: August 1, 2017)

By using a newly developed di-nuclear system model with a dynamical potential energy surface—the DNS-DyPES model, hot fusion reactions for synthesizing superheavy nuclei (SHN) with the charge number $Z = 112$–120 are studied. The calculated evaporation residue cross sections are in good agreement with available data. In the reaction ^{50}Ti+^{249}Bk $\rightarrow$ $^{299-x}$119 + xn, the maximal evaporation residue (ER) cross section is found to be about 0.11 pb for the 4n-emission channel. For projectile-target combinations producing SHN with $Z = 120$, the ER cross section increases with the mass asymmetry in the incident channel increasing. The maximal ER cross sections for ^{58}Fe+^{244}Pu and ^{54}Cr+^{248}Cm are relatively small (less than 0.01 pb) and those for ^{50}Ti+^{249}Cf and ^{50}Ti+^{251}Cf are about 0.05 and 0.25 pb, respectively.

PACS numbers: 24.10.-i, 25.70.Jj, 24.60.Dr, 27.90.+b

In the last decades, a lot of experimental progresses have been made in synthesizing superheavy elements (SHE). Up to now, SHEs with charge number $Z \leq 118$ have been produced via cold fusion reactions with Pb or Bi as targets [1, 2] and hot fusion reactions with ^{48}Ca as projectiles [3, 4]. There have been also some attempts to synthesize superheavy nuclei (SHN) with $Z > 118$. For example, experiments with projectile-target combinations ^{58}Fe+^{244}Pu [5] and ^{50}Ti+^{249}Cf [6] have been performed in order to produce the element 120 but no α decay chains consistent with fusion-evaporation reaction products were observed.

The evaporation residue (ER) cross section $\sigma_{\rm ER}$ of fusion reactions depends strongly on the projectile-target combination and the incident energy. The study of such dependences is interesting and useful particularly when one tries to synthesize new SHEs with $Z > 118$ because $\sigma_{\rm ER}$ of reactions with these nuclei as evaporation residues becomes tiny which makes the experiment much more difficult. In recent years much effort has devoted to the investigation of the synthesis mechanism of SHN with $Z > 118$. Using a dinuclear system (DNS) model, Feng *et al.* calculated the cross sections of cold fusion reactions with isotopes of elements 119 and 120 as evaporation residues and the maximal $\sigma_{\rm ER}$ was predicted to be about 0.03 pb and 0.09 pb for elements 119 and 120, respectively [7]. Hot fusion reactions with ^{50}Ti as the projectile were studied extensively by using the DNS models [8–11], the fusion by diffusion models [12–15], and some other models [16, 17]. The optimal incident energy and the maximal $\sigma_{\rm ER}$ from different models or with different parameters vary very much. For example, $\sigma_{\rm ER}$ for the reaction ^{50}Ti+^{249}Cf $\rightarrow$ ^{296}120 + 3n ranges from 1.5 to 760 fb [11].

In this work, we will study hot fusion reactions producing SHN with $Z \geq 112$ and in particular the elements 119 and 120 using a newly developed DNS model with a dynamical potential energy surface (DyPES) [18, 19] (the model is termed as the DNS-DyPES model). The importance of dynamical deformations of fragments in dissipative heavy-ion collisions has been long known [20, 21]. The dynamical deformations of the projectile and the target in the entrance channel have been included in the DNS models [22–24] and they are crucial for calculating the local excitation energy of a DNS during the process of nucleon transfers. Quite recently, Huang *et al.* [25] developed a new DNS model which takes into account the dynamical deformations of each DNS. In that model, a three-dimensional master equation is solved with three variables, the deformations β_i ($i = 1$ and 2 for each nucleus in a DNS) and the mass asymmetry η. In order to i) take into account the influence of the dynamical deformations of nuclei in each DNS and ii) make the calculation easier, we treat the dynamical deformations in a more transparent and economic way in the DNS-DyPES model. The details of this model will be published elsewhere [19] and here we only discuss briefly how to include the dynamical deformation.

As usual, the evaporation residue cross section in a heavy-ion fusion reaction is calculated as the summation over all partial wave J,

$$\sigma_{\rm ER}(E_{\rm c.m.}) = \sum_J \sigma_{\rm cap}(E_{\rm c.m.}, J) P_{\rm CN}(E_{\rm c.m.}, J) \times W_{\rm sur}(E_{\rm c.m.}, J), \quad (1)$$

with $E_{\rm c.m.}$ the incident energy in the center of mass frame. In this work the capture cross section $\sigma_{\rm cap}$

* sgzhou@itp.ac.cn

is calculated with an empirical coupled channel approach [26, 27] and the survival probability $W_{\rm sur}$ is calculated using a statistic model [28, 29]. In the fusion process, an excited compound nucleus (CN) may be formed. We calculate the formation probability of a CN $P_{\rm CN}$ based on the DNS concept. The DNS concept was proposed by Volkov in order to describe the deep inelastic transfer process [30]. This concept was later used to study the competition between complete fusion and quasi-fission and to calculate the fusion probability in fusion reactions [31–33]. Based on the DNS concept, several models have been developed for the study of the synthesis mechanism of SHN (see [34–37] and references therein).

The basic idea of the DNS concept is that after the capture process, a DNS $(A_{\rm P}, A_{\rm T})$ in the entrance channel is formed. Then the DNS evolves via nucleon transfer along the mass asymmetry coordinate η instead of in the direction of the relative distance between the projectile and the target R. During the nucleon transfer process, any DNS (A_1, A_2) with $A_1 = 0, 1, \cdots, A_{\rm P} + A_{\rm T}$ and $A_2 = A_{\rm P} + A_{\rm T} - A_1$ may be formed. The evolution of the distribution function of each DNS with time can be described by a master equation [22–24],

$$\frac{dP(A_1,t)}{dt} = \sum_{A_1'} W_{A_1A_1'}(t)\left[d_{A_1}(t)P(A_1',t) - d_{A_1'}(t)P(A_1,t)\right] - \Lambda^{\rm qf}_{A_1}(t)P(A_1,t). \quad (2)$$

Since $A_1+A_2 = A_{\rm P}+A_{\rm T}$, only A_1 is explicitly included in the above equation. $d_{A_1}(t)$ is the microscopic dimension for a DNS (A_1, A_2) with a local excitation energy $E^*_{\rm DNS}$ defined in Eq. (3). $E^*_{\rm DNS}$ is shared by the two nuclei in this DNS. For each nucleus, a valence space is opened due to the excitation and those nucleons in the states within the valence space are active for the transfer between the two nuclei. $d_{A_1}(t) = C^{N_1}_{m_1}C^{N_2}_{m_2}$ where N_k is the number of valence states and m_k is that of valence nucleons [22]. $\Lambda^{\rm qf}_{A_1}$ is the quasifission probability of the DNS (A_1, A_2) and $W_{A_1A_1'}(t) = W_{A_1'A_1}(t)$ is the mean transition probability between the DNS's (A_1, A_2) and (A_1', A_2'). For the details about how to solve the master equation, please refer to Refs. [22–24]. Here we only focus on the local excitation energy and the dynamical deformations.

In Eq. (2), $d_{A_1}(t)$, $\Lambda^{\rm qf}_{A_1}$, and $W_{A_1A_1'}(t)$ all depend on the local excitation energy of the DNS,

$$E^*_{\rm DNS}(A_1,t) = E_{\rm total} - E^0_{\rm DNS}(A_1,t) - E^{\rm rot}_{\rm DNS}(t), \quad (3)$$

with

$$E_{\rm total} = E_{\rm c.m.} + (M_{\rm T} + M_{\rm P})c^2, \quad (4)$$

$$E^0_{\rm DNS}(A_1,t) = V_{\rm DNS}(A_1,t) + (M_1 + M_2)c^2, \quad (5)$$

$$E^{\rm rot}_{\rm DNS}(t) = \frac{J(J+1)}{2\mathcal{J}_{\rm DNS}(A_1,t)}. \quad (6)$$

$V_{\rm DNS}(A_1,t) = V_{\rm N}(A_1,t) + V_{\rm C}(A_1,t)$ and $V_{\rm N}(A_1,t)$ and $V_{\rm C}(A_1,t)$ are the nuclear and the Coulomb interactions between the two nuclei. The potential energy in the mass asymmetry degree of freedom, which is often called as the driving potential at $t = 0$, is defined as

$$V_{\rm PES}(A_1,t) \equiv V_{\rm DNS}(A_1,t) + (M_1 + M_2 - M_{\rm T} - M_{\rm P})c^2. \quad (7)$$

The interaction potential $V_{\rm DNS}(A_1,R,t)$ between the two nuclei in a DNS depends on the distance between their centers R and $V_{\rm DNS}(A_1,t)$ in Eqs. (5) and (7) takes the minimum value of the pocket with respect to R in $V_{\rm DNS}(A_1,R,t)$, *i.e.*, $V_{\rm DNS}(A_1,t) \equiv V_{\rm DNS}(A_1,R,t)|_{R=R_{\rm pocket}}$.

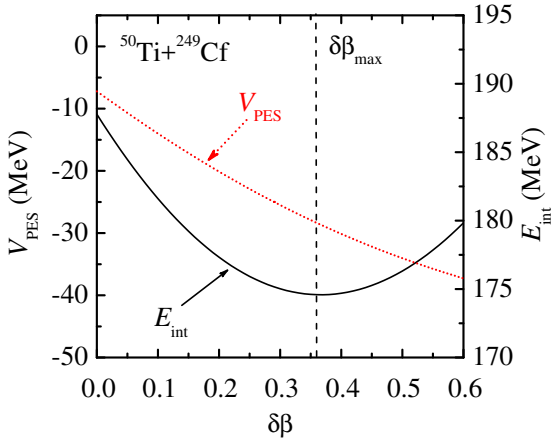

FIG. 1. (Color online) The total "intrinsic" energy $E_{\rm int}$ (the black solid curve) and the potential energy $V_{\rm PES}$ (the red dotted curve) as a function of the dynamical deformation $\delta\beta$ for the projectile-target combination ^{50}Ti + ^{249}Cf. The vertical dashed line shows the maximal dynamical deformation $\delta\beta_{\rm max}$.

Due to the attractive nuclear force and the repulsive Coulomb force, both nuclei in a DNS are distorted and dynamical deformations develop during the process of nuclear transfers [20, 21]. This results in the time-dependence of the potential energy surface (PES). The nuclear interaction is calculated with a double-folding method [38] and the Coulomb interaction from the Wong formula [39]. In this work we assume a tip-tip orientation of the two deformed nuclei and that the dynamical deformations of the two nuclei satisfy $\delta\beta_1^2 C_1/A_1 = \delta\beta_2^2 C_2/A_2$ [26] with the stiffness parameter C_i ($i = 1$ and 2) calculated from a liquid drop model [40]. We then define $\delta\beta \equiv (\delta\beta_1 + \delta\beta_2)/2$ and following Refs. [20, 21] we assume that the dynamical deformation evolves in an

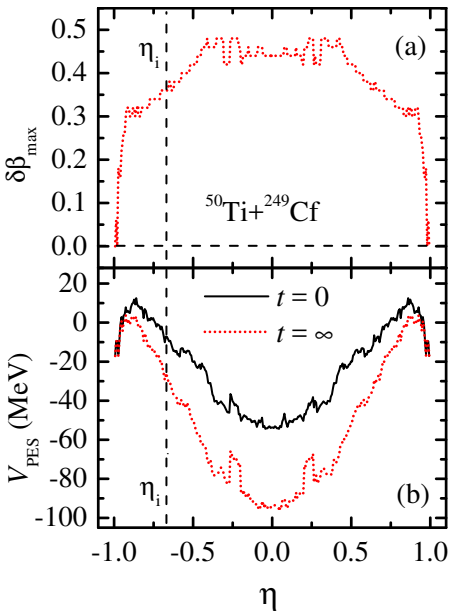

FIG. 2. (Color online) (a) The maximal dynamical deformation $\delta\beta_{\rm max}$ and (b) the dynamical potential energy surface (DyPES) defined in Eq. (7) at $t = 0$ and $t = \infty$ as functions of the mass asymmetry coordinate η for the projectile-target combination ^{50}Ti + ^{249}Cf. The vertical dashed line shows the entrance channel.

overdamped motion,

$$\delta\beta(t) = \delta\beta_{\rm max}\left(1 - e^{-t/\tau_{\rm def}}\right), \tag{8}$$

where the relaxation time $\tau_{\rm def} = 40 \times 10^{-22}$ s [21] and the maximal dynamical deformation $\delta\beta_{\rm max}$ is determined by minimizing the total "intrinsic" energy,

$$E_{\rm int}(A_1, \delta\beta) = V_{\rm N}(A_1; \beta_1, \beta_2) + V_{\rm C}(A_1; \beta_1, \beta_2) + \sum_{i=1,2} \frac{1}{2} C_i \delta\beta_i^2, \tag{9}$$

where the quadrupole deformation $\beta_i = \beta_i^0 + \delta\beta_i$ ($i = 1$ and 2) with the static deformation parameters β_i^0 taken from Ref. [41]. This is illustrated for ^{50}Ti + ^{249}Cf in Fig. 1 (the black solid curve) where one finds that with $\delta\beta$ increasing, $E_{\rm int}$ decreases and takes the minimal value at $\delta\beta \sim 0.36$.

Figure 2 shows the maximal dynamical deformation $\delta\beta_{\rm max}$ and the DyPES defined in Eq. (7) at $t = 0$ and $t = \infty$ as functions of the mass asymmetry coordinate $\eta \equiv (A_1 - A_2)/(A_1 + A_2)$ for ^{50}Ti + ^{249}Cf. The values of nuclear masses are taken from Refs. [41, 42]. In general, with the mass asymmetry increasing, the maximal dynamical deformation becomes smaller and when η approaches to ± 1, which corresponds to the formation of a CN, $\delta\beta_{\rm max}$ approaches to zero. The local excitation energy becomes larger when the dynamical deformation develops. For those DNS's with larger values of $\delta\beta_{\rm max}$, the gain of local excitation energy, $\delta V_{\rm PES}^{\rm max}(A_1) \equiv V_{\rm PES}(A_1, t = 0) - V_{\rm PES}(A_1, t = \infty)$, is also larger. Note that, since $\delta\beta_{\rm max}$ for $\eta = \pm 1$ is zero, the local excitation energy of the CN $E_{\rm CN}^*$ is always fixed and $E_{\rm CN}^* = Q + E_{\rm c.m.}$ with Q the reaction energy. In Fig. 1 we plot the potential energy $V_{\rm PES}$ (the red dotted curve) as a function of $\delta\beta$ for ^{50}Ti + ^{249}Cf. It can be seen that the potential energy decreases almost linearly with the dynamical deformation increasing. Therefore, in order to reduce the numerical time, we assume

$$V_{\rm PES}(A_1, t) = V_{\rm PES}(A_1, t = 0) - \frac{\delta\beta(t)}{\delta\beta_{\rm max}} \delta V_{\rm PES}^{\rm max}(A_1). \tag{10}$$

Note that a dynamical PES has been calculated microscopically to describe a continuous transition from the initial diabatic potential to the asymptotic adiabatic one due to a residual two-body collision [43, 44]. It would be an interesting topic to explore the connection between the DyPES in the present work and that proposed in Refs. [43, 44].

With the DNS-DyPES model, we studied systematically hot fusion reactions producing superheavy nuclei with the charge number $Z = 112$–120. In Fig. 3, maximal values of experimentally available evaporation residue cross sections for ^{48}Ca induced reactions leading to SHN with $Z = 112$–118 [4, 45–47] are compared with the theoretical values calculated at the incident energy in the center of mass frame $E_{\rm c.m.}$ which are indicated in the plot. The calculated maximal evaporation residue cross sections for ^{50}Ti induced reactions leading to SHN with $Z = 119$ and 120 are also shown. For reactions leading to SHN with $Z = 112$–118, the projectile is ^{48}Ca and targets are ^{238}U, ^{237}Np, ^{242}Pu, ^{243}Am, ^{248}Cm, ^{249}Bk, and ^{249}Cf, respectively. For SHN with $Z = 113$, 115, and 118,

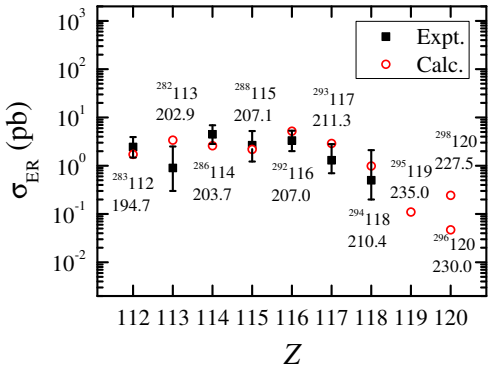

FIG. 3. (Color online) Maximal values of experimentally available evaporation residue cross sections for ^{48}Ca induced reactions leading to SHN with $Z = 112$–118 compared with the theoretical values calculated at the incident energy in the center of mass frame $E_{\rm c.m.}$ (in MeV) which are indicated in the plot. The calculated maximal evaporation residue cross sections for ^{50}Ti induced reactions leading to SHN with $Z = 119$ and 120 are also shown. For each superheavy nucleus, the charge and mass numbers are given and the experimental values are shown by black solid squares with error bars and the theoretical ones by red open circles.

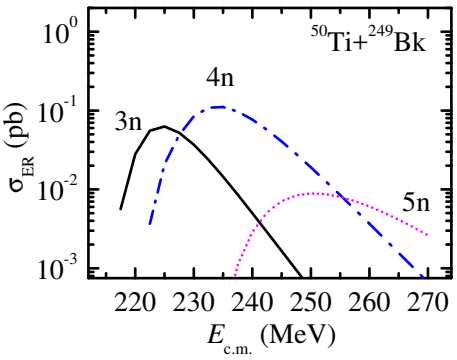

FIG. 4. (Color online) Evaporation residue cross sections σ_{ER} as a function of the incident energy in the center of mass frame $E_{c.m.}$ for the reaction ^{50}Ti+^{249}Bk.

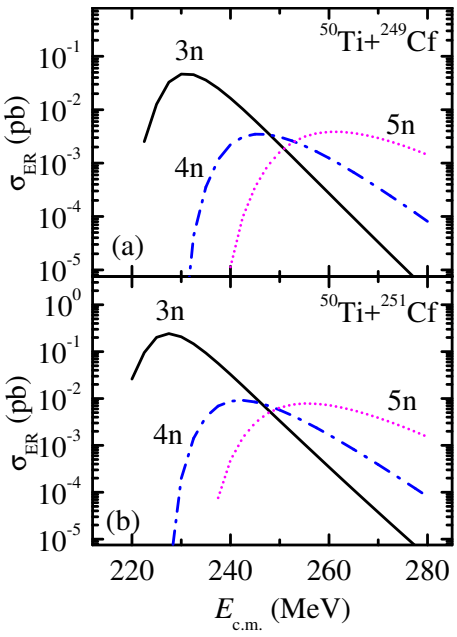

FIG. 5. (Color online) Evaporation residue cross sections σ_{ER} as a function of the incident energy in the center of mass frame $E_{c.m.}$ for (a) ^{50}Ti+^{249}Cf (b) and ^{50}Ti+^{251}Cf.

the maximal σ_{ER} is found in the 3n evaporation residue channel and for those with $Z = 114$, 116, and 117, the 4n channel is more favorable. For the element 112, according to our calculation, the ER cross section in the 4n channel leading to ^{282}Cn is a bit larger than that in the 3n channel. But the maximal σ_{ER} is found in the 3n channel in the experiment and in Fig. 3 the calculated and experimental results for ^{283}Cn are given. From Fig. 3, one finds a good agreement between the calculation and the experiment. We note that the inclusion of the DyPES in this work reduces by about an order of magnitude the fusion probability and the ER cross section.

From $Z = 112$ to 116, the experimental cross section staggers and the values are between 1 to 10 pb. For $Z > 116$, the ER cross section decreases almost exponentially with the charge number increasing. A similar trend is also found in the calculated results for SHN with $Z = 112$–118. Whether this trend continues or not is a very interesting question. The maximal ER cross sections for the SHN ^{296}119 in ^{50}Ti + ^{249}Bk, ^{296}120 in ^{50}Ti + ^{249}Cf (the lower circle), and ^{298}120 in ^{50}Ti + ^{251}Cf (the upper circle) are also shown in Fig. 3. It can be seen that, for the element 119, the decreasing tendency in the ER cross section continues after $Z = 118$ and the ER cross section is about 0.11 pb. This tendency continues also for the element 120 if ^{249}Cf is used as the target and the ER cross section is only about 0.05 pb. However, for the 3n-emission channel of ^{50}Ti + ^{251}Cf, which produces ^{298}120, the maximal ER cross section is about 0.25 pb.

The synthesis of isotopes of the element 119 with ^{50}Ti as the projectile has been investigated extensively from the theoretical side. As we mentioned earlier, the maximal σ_{ER} from different models or with different parameters vary very much. Let's take the projectile-target combination ^{50}Ti+^{249}Bk as an example. The maximal σ_{ER} varies from 35 [17], 50 [16], and up to 570 fb [15]. In this work, the production cross sections for the synthesis of the element 119 are studied with the DNS-DyPES model. The excitation functions for ^{50}Ti + ^{249}Bk leading to $^{294-296}$119 are represented by solid, dash dot and dotted curves in Fig. 4. The maximal cross sections for 3n and 4n channels are found to be about 0.06 and 0.11 pb, respectively.

In an attempt to synthesize SHN with $Z = 120$ using the projectile-target combination ^{58}Fe + ^{244}Pu, no decay chains consistent with fusion-evaporation reaction products were observed [5]. According to the sensitivity of this experiment, the null result sets an upper limit of 0.4 pb for σ_{ER}. Some predictions have been made for the ER cross section for this reaction. For example, the maximal σ_{ER} is predicted to be about 0.1 pb in the 3n channel in Ref. [8] and about 0.003 pb in the 4n channel in Ref. [17]. In this work, the ER cross section in the 4n channel is larger and the maximal value is only about 4 fb which is far below the current experimental limit. By examining the excitation function for a more asymmetric projectile-target combination, ^{54}Cr + ^{248}Cm, we find that the maximal cross section is also very small and is only about 6 fb in the 4n channel which is similar to the results of Ref. [17].

Next we investigate ^{50}Ti induced reactions for the synthesis of isotopes of the SHE with $Z = 120$. The excitation functions for ^{50}Ti + ^{249}Cf and ^{50}Ti + ^{251}Cf are shown in Fig. 5. In both cases the 3n-emission channel gives larger ER cross sections than does the 4n channel due to the odd-even effects in the survival probability. It is found that the maximal cross section for ^{50}Ti + ^{249}Cf is about 0.05 pb. However, for ^{50}Ti + ^{251}Cf, the ER cross section can be as large as 0.25 pb which is close to the current experiment limit. The reason for a large ER cross section in these two reactions is that the fusion probability increases considerably with the mass asymmetry

increasing; the fusion probabilities for ^{50}Ti + ^{249,251}Cf are about one order of magnitude larger than that for ^{58}Fe + ^{244}Pu [19].

In summary, we developed a di-nuclear system (DNS) model with a dynamical potential energy surface (DyPES)—the DNS-DyPES model. In this model, the development of dynamical deformations of the two nuclei in a DNS is approximately taken into account. This is crucial for the determination of the local excitation energy of DNS's involved in the fusion process. With the DNS-DyPES model, heavy ion fusion reactions with trans-uranium nuclei as targets are investigated. The calculated evaporation residue (ER) cross sections are in good agreement with available experimental values for the reactions producing superheavy nuclei with Z =112–118. The projectile-target combination ^{50}Ti+^{249}Bk for synthesizing the element 119 is studied and the maximal ER cross section is found to be about 0.11 pb for the 4n-emission channel. For projectile-target combinations which lead to the synthesis of SHN with $Z = 120$, the ER cross section increases with the mass asymmetry of the entrance channel increasing. The ER cross sections for ^{58}Fe+^{244}Pu and ^{54}Cr+^{248}Cm are relatively small (less than 10 fb) and those for ^{50}Ti+^{249}Cf and ^{50}Ti+^{251}Cf are about 0.05 and 0.25 pb, respectively.

We thank Professor Jun-Qing Li for helpful discussions. The work was supported by NSF China (10975100, 10979066, 11175252, and 11120101005), MOST of China (2007CB815000), the Knowledge Innovation Project of CAS (KJCX2-EW-N01 and KJCX2-YW-N32), and Deutsche Forschungsgemeinschaft (DFG). N.W., E.G.Z., and S.G.Z. would like to express their gratitude to W. Scheid for the kind hospitality extended to them at Giessen University where part of this work was done under the support of NSF China and DFG. Part of the numerical results is obtained on the ScGrid of Supercomputing Center, CNIC of CAS.

[1] S. Hofmann and G. Münzenberg, Rev. Mod. Phys. **72**, 733 (2000).
[2] K. Morita, K. Morimoto, D. Kaji, T. Akiyama, S.-i. Goto, H. Haba, E. Ideguchi, R. Kanungo, K. Katori, H. Koura, H. Kudo, T. Ohnishi, A. Ozawa, T. Suda, K. Sueki, H.-S. Xu, T. Yamaguchi, A. Yoneda, A. Yoshida, and Y.-L. Zhao, J. Phys. Soc. Jpn. **73**, 2593 (2004).
[3] Y. Oganessian, J. Phys. G: Nucl. Phys. **34**, R165 (2007).
[4] Y. T. Oganessian, F. S. Abdullin, P. D. Bailey, D. E. Benker, M. E. Bennett, S. N. Dmitriev, J. G. Ezold, J. H. Hamilton, R. A. Henderson, M. G. Itkis, Y. V. Lobanov, A. N. Mezentsev, K. J. Moody, S. L. Nelson, A. N. Polyakov, C. E. Porter, A. V. Ramayya, F. D. Riley, J. B. Roberto, M. A. Ryabinin, K. P. Rykaczewski, R. N. Sagaidak, D. A. Shaughnessy, I. V. Shirokovsky, M. A. Stoyer, V. G. Subbotin, R. Sudowe, A. M. Sukhov, Y. S. Tsyganov, V. K. Utyonkov, A. A. Voinov, G. K. Vostokin, and P. A. Wilk, Phys. Rev. Lett. **104**, 142502 (2010).
[5] Y. T. Oganessian, V. K. Utyonkov, Y. V. Lobanov, F. S. Abdullin, A. N. Polyakov, R. N. Sagaidak, I. V. Shirokovsky, Y. S. Tsyganov, A. A. Voinov, A. N. Mezentsev, V. G. Subbotin, A. M. Sukhov, K. Subotic, V. I. Zagrebaev, S. N. Dmitriev, R. A. Henderson, K. J. Moody, J. M. Kenneally, J. H. Landrum, D. A. Shaughnessy, M. A. Stoyer, N. J. Stoyer, and P. A. Wilk, Phys. Rev. C **79**, 024603 (2009).
[6] C. E. Dullmann, "News from TASCA," talk given at the 10th Workshop on Recoil Separator for Superheavy Element Chemistry, October 14, 2011, GSI Darmstadt, Germany.
[7] Z.-Q. Feng, G.-M. Jin, J.-Q. Li, and W. Scheid, Phys. Rev. C **76**, 044606 (2007).
[8] A. K. Nasirov, G. Giardina, G. Mandaglio, M. Manganaro, F. Hanappe, S. Heinz, S. Hofmann, A. I. Muminov, and W. Scheid, Phys. Rev. C **79**, 024606 (2009).
[9] G. Adamian, N. Antonenko, and W. Scheid, Eur. Phys. J. A **41**, 235 (2009).
[10] Z.-G. Gan, X.-H. Zhou, M.-H. Huang, Z.-Q. Feng, and J.-Q. Li, Sci. China-Phys. Mech. Astron. **54 (Supp. 1)**, s61 (2011).
[11] A. K. Nasirov, G. Mandaglio, G. Giardina, A. Sobiczewski, and A. I. Muminov, Phys. Rev. C **84**, 044612 (2011).
[12] Z. H. Liu and J.-D. Bao, Phys. Rev. C **80**, 054608 (2009).
[13] K. Siwek-Wilczynska, T. Cap, and J. Wilczynski, Int. J. Mod. Phys. E **19**, 500 (2010).
[14] Z.-H. Liu and J.-D. Bao, Phys. Rev. C **83**, 044613 (2011).
[15] Z.-H. Liu and J.-D. Bao, Phys. Rev. C **84**, 031602(R) (2011).
[16] V. Zagrebaev and W. Greiner, Phys. Rev. C **78**, 034610 (2008).
[17] N. Wang, J. Tian, and W. Scheid, Phys. Rev. C **84**, 061601(R) (2011).
[18] S.-G. Zhou, "A dinulcear system model for fusion reactions with consistent and effective coupled-channel effects," seminar given at Giessen University, April 16, 2010.
[19] N. Wang *et al.*, in preparation.
[20] C. Riedel, G. Wolschin, and W. Noerenberg, Z. Phys. A **290**, 47 (1979); C. Riedel and W. Nörenberg, Z. Phys. A **290**, 385 (1979).
[21] G. Wolschin, Phys. Lett. B **88**, 35 (1979).
[22] W. Li, N. Wang, J. F. Li, H. Xu, W. Zuo, E. Zhao, J. Q. Li, and W. Scheid, Europhys. Lett. **64**, 750 (2003).
[23] W. Li, N. Wang, F. Jia, H. Xu, W. Zuo, Q. Li, E. Zhao, J. Li, and W. Scheid, J. Phys. G: Nucl. Phys. **32**, 1143 (2006).
[24] N. Wang, J.-Q. Li, and E.-G. Zhao, Phys. Rev. C **78**, 054607 (2008).
[25] M. Huang, Z. Zhang, Z. Gan, X. Zhou, J. Li, and W. Scheid, Phys. Rev. C **84**, 064619 (2011).
[26] V. I. Zagrebaev, Phys. Rev. C **64**, 034606 (2001).
[27] Z.-Q. Feng, G.-M. Jin, F. Fu, and J.-Q. Li, Nucl. Phys. A **771**, 50 (2006).
[28] A. S. Zubov, G. G. Adamian, N. V. Antonenko, S. P. Ivanova, and W. Scheid, Phys. Rev. C **65**, 024308 (2002).

[29] C.-J. Xia, B.-X. Sun, E.-G. Zhao, and S.-G. Zhou, Sci. China-Phys. Mech. Astron. **54 (Suppl. 1)**, 109 (2011), arXiv: 1101.2725 [nucl-th].
[30] V. V. Volkov, Phys. Rep. **44**, 93 (1978).
[31] N. Antonenko, E. Cherepanov, A. Nasirov, V. Permjakov, and V. Volkov, Phys. Lett. B **319**, 425 (1993).
[32] N. V. Antonenko, E. A. Cherepanov, A. K. Nasirov, V. P. Permjakov, and V. V. Volkov, Phys. Rev. C **51**, 2635 (1995).
[33] G. G. Adamian, N. V. Antonenko, W. Scheid, and V. V. Volkov, Nucl. Phys. A **627**, 361 (1997).
[34] E. G. Zhao, N. Wang, Z. Q. Feng, J. Q. Li, S. G. Zhou, and W. Scheid, Int. J. Mod. Phys. E **17**, 1937 (2008).
[35] A. Zubov, G. Adamian, and N. Antonenko, Phys. Part. Nucl. **40**, 847 (2009).
[36] J.-Q. Li, Z.-Q. Feng, Z.-G. Gan, X.-H. Zhou, H.-F. Zhang, and W. Scheid, Nucl. Phys. A **834**, 353c (2010).
[37] Z.-Q. Feng, G.-M. Jin, and J.-Q. Li, Nucl. Phys. Rev. **28**, 1 (2011).
[38] G. G. Adamian, N. V. Antonenko, R. V. Jolos, S. P. Ivanova, and O. I. Melnikova, Int. J. Mod. Phys. E **5**, 191 (1996).
[39] C. Y. Wong, Phys. Rev. Lett. **31**, 766 (1973).
[40] W. D. Myers and W. J. Swiatecki, Nucl. Phys. **81**, 1 (1966).
[41] P. Möller, J. R. Nix, W. D. Myers, and W. J. Swiatecki, At. Data Nucl. Data Tables **59**, 185 (1995).
[42] G. Audi, A. H. Wapstra, and C. Thibault, Nucl. Phys. A **729**, 337 (2003).
[43] A. Diaz-Torres, Phys. Rev. C **69**, 021603(R) (2004).
[44] A. Diaz-Torres, Phys. Rev. C **74**, 064601 (2006).
[45] V. I. Zagrebaev, A. S. Denikin, A. V. Karpov, A. P. Alekseev, V. V. Samarin, V. A. Rachkov, and M. A. Naumenko, "Low-energy nuclear knowledge base (Nuclear Reaction Video)," `http://nrv.jinr.ru/nrv/`.
[46] Y. T. Oganessian, V. K. Utyonkov, Y. V. Lobanov, F. S. Abdullin, A. N. Polyakov, R. N. Sagaidak, I. V. Shirokovsky, Y. S. Tsyganov, A. A. Voinov, G. G. Gulbekian, S. L. Bogomolov, B. N. Gikal, A. N. Mezentsev, V. G. Subbotin, A. M. Sukhov, K. Subotic, V. I. Zagrebaev, G. K. Vostokin, M. G. Itkis, R. A. Henderson, J. M. Kenneally, J. H. Landrum, K. J. Moody, D. A. Shaughnessy, M. A. Stoyer, N. J. Stoyer, and P. A. Wilk, Phys. Rev. C **76**, 011601(R) (2007).
[47] Y. T. Oganessian, V. K. Utyonkov, Y. V. Lobanov, F. S. Abdullin, A. N. Polyakov, R. N. Sagaidak, I. V. Shirokovsky, Y. S. Tsyganov, A. A. Voinov, G. G. Gulbekian, S. L. Bogomolov, B. N. Gikal, A. N. Mezentsev, S. Iliev, V. G. Subbotin, A. M. Sukhov, K. Subotic, V. I. Zagrebaev, G. K. Vostokin, M. G. Itkis, K. J. Moody, J. B. Patin, D. A. Shaughnessy, M. A. Stoyer, N. J. Stoyer, P. A. Wilk, J. M. Kenneally, J. H. Landrum, J. F. Wild, and R. W. Lougheed, Phys. Rev. C **74**, 044602 (2006).